Nanotechnology **20** (2009) 285310 (5pp) doi:10.1088/0957-4484/20/28/285310

The fabrication of periodic metal nanodot arrays through pulsed laser melting induced fragmentation of metal nanogratings

Qiangfei Xia and Stephen Y Chou[1]

Nanostructure Laboratory, Department of Electrical Engineering, Princeton University, Princeton, NJ 08544, USA

E-mail: chou@princeton.edu

Received 16 March 2009, in final form 29 April 2009
Published 23 June 2009
Online at stacks.iop.org/Nano/20/285310

Abstract

We propose and demonstrate a new method for fabricating periodic arrays of metal nanodots over a large area. In this method, metal nanogratings were first patterned on a substrate by nanoimprint lithography and lift-off, and were then melted using a single excimer laser pulse. We found that the laser melting broke the metal nanogratings into periodic nanodots. Furthermore, we demonstrated the control of the nanodot array pitch using a substrate surface topology, and the fabrication of two-dimensional periodic metal nanodot arrays of 70 nm diameter and 200 nm period. The fragmentation of lines into dots was attributed to the Rayleigh instability in a liquid cylinder.

(Some figures in this article are in colour only in the electronic version)

Metal nanodots have wide applications in catalysis [1], environmental remediation [2], DNA detection [3], high density data storage [4], and electronic and optical devices [5, 6]. In certain applications, periodic 1D or 2D arrays of nanodots are required. The common methods used today for fabricating metal nanodot arrays are either self-assembly based wet chemical processes or lithography based nanopatterning. The self-assembly methods include drop-casting [4] and spin-coating [7] of nanodot colloidal solutions on a substrate followed by solvent evaporation; self-assembly using a Langmuir–Blodgett technique [8]; templated self-assembly from nanodot colloids using templates such as biomolecules [9, 10]; and template-free self-assembly methods such as oriented aggregation [11], to name a few. Templated self-assembly offers nanometer precision and high throughput, but the nanoparticles have to be biocompatible or water soluble. In some cases, an additional step of a high-temperature thermal annealing is required to improve the adhesion between the particles and the substrate [4], which not only further increases the cost, but also is incompatible with substrates like plastics that cannot withstand high temperatures. On the other hand, lithography tools such as electron beam lithography (EBL) [12] and focus ion beam [13] allow well defined and well positioned nanodots, but they are limited by low throughput and small areas.

In this paper, we propose and demonstrate a simple method that has a great potential to manufacture periodic metal nanodot arrays over large areas with low costs. Our method, termed melting induced fragmentation (MIF), starts with patterning of metal gratings by nanoimprint lithography (NIL) and a metal lift-off [14, 15]. The metal nanogratings are then fragmented into arrays of round and periodic metal nanodots by a single laser pulse melting, favoring the minimum surface energy [16, 17]. Previously, a laser melting was used to change the shape of metal islands on a quartz substrate into spherical nanodots [18–21]. However, in those cases there was no patterning on the metal thin films and usually multiple laser pulses were used for their processes.

To fabricate the metal nanogratings used in MIF, NIL was first carried out to define a nanograting pattern in a resist on a substrate. After removing the residual resist layer by reactive ion etching (RIE), a metal thin film was deposited

[1] Author to whom any correspondence should be addressed.

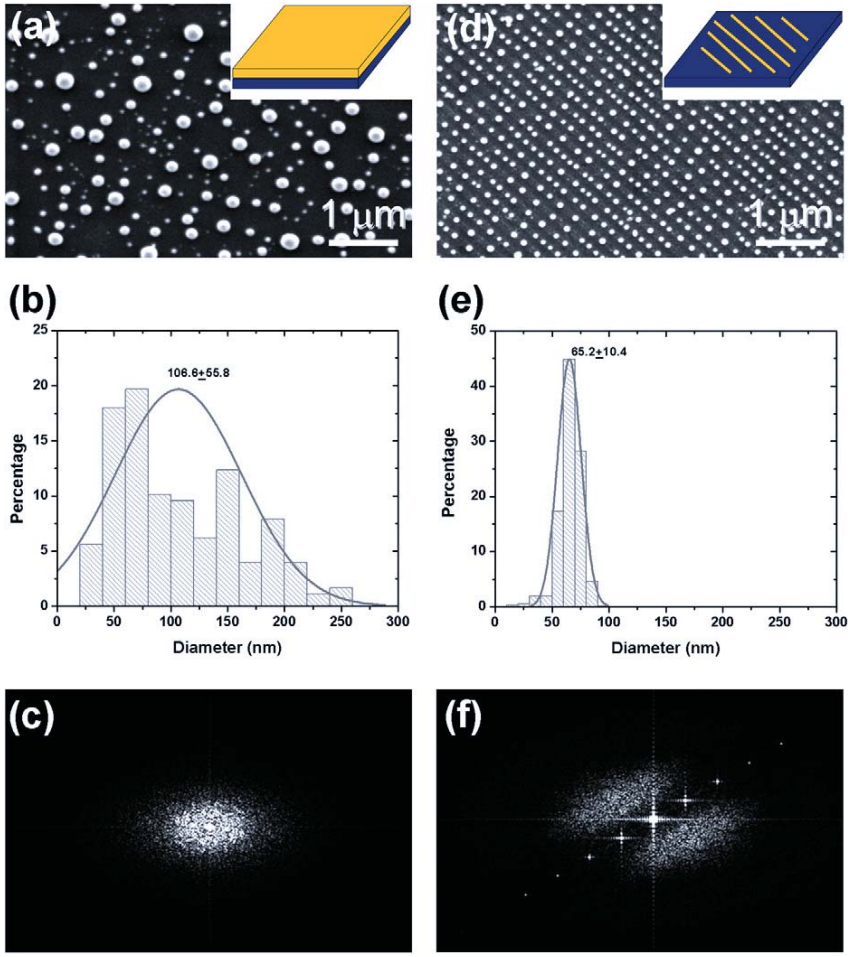

Figure 1. Au nanodots formed by fragmentation of a blank thin film (left column) and a 200 nm pitch, 100 nm line width grating (right column) on fused silica substrates. (a) SEM image of nanodots from a continuous film; (b) histogram of the particle size distribution for (a), the size is 106.6 ± 55.8 nm; (c) FFT image for (a), showing no regular periodicity for the particles in (a); (d) SEM image of nanodots from Au lines; (e) histogram of the particle size distribution for (d), the size is 65.2 ± 10.4 nm; (f) FFT image for (d), showing a periodicity of 220 ± 70 nm along the original grating line direction and the original 200 ± 9 nm grating period in the orthogonal direction. In both cases the films are 10 nm thick (with 2 nm Ti adhesion layer), and the laser fluences are 194 mJ cm^{-2}. Insets in (a) and (d) are schematics of the starting structures (blank thin film and nanogratings) on substrates.

on the substrates (fused silica or Si with thermal oxide) using an electron beam evaporator, followed by a lift-off process in warm acetone. The fabricated metal nanogratings (for example, 10 nm thick Au with 2 nm Ti adhesion layer) had 200 nm pitch and 70–100 nm line width. For comparison, we also prepared a blank Au thin film (10 nm Au/2 nm Ti) on a fused silica substrate.

To fragment the metal grating into nanodots, a single XeCl laser pulse (308 nm wavelength, 20 ns pulse width, 3×3 mm^2 spot size) was used to melt the gratings. To characterize the metal nanodots fabricated, we took scanning electron microscope (SEM) images first, then analyzed them using a commercial image analysis software (Image Pro-Plus) [22] to gain the size and spacing distribution information of the nanodots.

Our experiments showed that on a flat surface of a substrate the nanodot arrays fabricated by MIF of metal nanogratings had far more uniform size distribution and periodicity than those from a blank thin film. For instance, a single laser pulse (194 mJ cm^{-2}) melting of the 10 nm Au/2 nm Ti blank film on fused silica broke the film into particles with an average diameter of 106.6 ± 55.8 nm and a broad distribution of period (figures 1(a)–(c)). However, with the same laser fluence, the diameter of the nanodots formed from the 200 nm pitch gratings (10 nm Au/2 nm Ti on fused silica) was 65.2 ± 10.4 nm, with a period of 220 ± 70 nm along the original grating line direction and a period of 200 ± 9 nm (the same as the original grating period) in the orthogonal direction (figures 1(d)–(f)). The relative standard variations (1 sigma) of the size and pitch distribution were significantly better than those of nanodots from a blank thin film. It is worth pointing out that previously we have shown that the final dot size is dependent on factors such as the film thickness, the linewidth, etc [16, 23].

To improve the nanodot periodicity in the original grating direction, we further propose to use pre-patterned substrates.

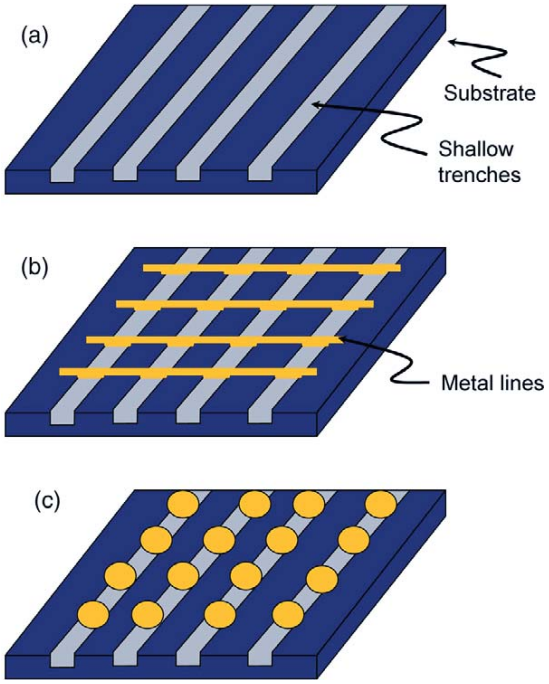

Figure 2. Principle of periodicity engineering using surface topography. (a) Patterning of shallow trenches on a substrate; (b) metal lines are patterned and deposited with an angle (adjustable) to the trench direction; (c) during the fragmentation process, the molten particle material flows into the trenches and resolidifies at the cross points of the trench and the metal lines due to a lower energy on those sites, forming an array with regular pitch.

For example, we pre-patterned the substrates with shallow trenches (10 nm deep, 70 nm wide, and 200 nm pitch) using NIL and RIE (figure 2(a)). The metal gratings were made normal to the pre-patterned grating (figure 2(b)). Particularly, we made samples as follows: (a) 10 nm Au/2 nm Ti gratings of 200 nm pitch and 100 nm linewidth on a pre-patterned fused silica wafer; and (b) 7 nm thick permalloy gratings of 200 nm pitch and 70 nm linewidth on a pre-patterned Si wafer with 210 nm thick thermal oxide. During the fragmentation process, the molten material tends to flow into the trench/wire cross points to minimize the system energy. As a result, the nanodots period along the original nanograting line direction is determined by the period of the shallow trenches rather than the natural MIF on a blank substrate (figure 2(c)).

The nanogratings on pre-patterned substrates were exposed to single laser pulses with fluences of 325 mJ cm^{-2} for Au and 790 mJ cm^{-2} for permalloy, respectively. Again periodic arrays of metal nanodots were formed on the substrates (figures 3(a) and (c)). A closer examination on the SEM images (insets, figures 3(a) and (c)) indicated that the resultant nanodots were sitting in the cross points of the original metal lines and the shallow trenches, favoring minimum system energy. The fast Fourier transfer (FFT) analysis showed the periodicity of nanodots in the original metal line direction was 200.0 ± 11.3 nm and in the normal direction was 200.0 ± 6.9 nm (figure 3(b)) for Au, and those for permalloy were 200.0 ± 7.4 nm and 200.0 ± 5.8 nm, respectively (figure 3(d)). Compared with the nanodot arrays by fragmentation of a blank Au film (figures 1(a) and (c)) (which had no certain periodicity), and those by fragmentation of Au nanogratings on a flat surface (figures 1(d) and (f)) (which had a pitch of 220 ± 70 nm in the original grating line direction), the pitches of the nanodot arrays in figure 3 were much more uniform because they were predetermined by the pitches of the shallow trenches on the substrate surface and the original metal nanogratings. It has to be pointed out that in figure 3, the permalloy has a more uniform periodicity than Au in both directions. There are also some missing dots in the Au nanodots array and some cloud in the FFT image (figures 3(a) and (b)), this could be due to the migration of Au at molten state because it has higher mobility.

The laser fragmentation process can be explained using Rayleigh instability theory, which predicts that a liquid cylinder of a radius R will become unstable and starts to break into periodic droplets of a critical wavelength, λ_c [24]. If it is perturbed along the cylinder longitudinal direction, the critical wavelength can be calculated using $\lambda_c = 2\pi R$ and the maximum (equilibrium) wavelength is $\lambda_m = 2\sqrt{2}\pi R$ [25]. With this model, first we can understand easily why a nanograting on a substrate can lead to periodic nanodots of uniform diameter while a blank thin film cannot. Second, we find the pitch of the nanodots along the original grating lines agrees with Rayleigh instability model. For example, 80 nm wide Cr lines of 200 nm pitch broke into the dots with an average period of about 250 nm along the original grating line direction (picture not shown in this text). The ratio of the nanodot pitch to the original grating line width is 3.12, which is close to the predicted value (π), suggesting that Rayleigh instability is the governing mechanism.

Although the pitch of nanodots depends heavily on the original nanowire width according to Rayleigh instability theory, they can be regulated using substrate surface topography, as shown in figure 3. The final nanostructure will be the determined by both the natural instability process and the substrate surface topography. Take figure 3 for instance, the pitch of the shallow trenches is 200 nm, smaller than the maximum instability wavelength ($2\sqrt{2}\pi R$), as a result, there was only one dot at each trench/grating intersection point. And the pitch of the nanodots along the original grating direction is determined by the original trench pitch. However, if the pitch of the surface relief structure is larger than the maximum wavelength $2\sqrt{2}\pi R$, one shall expect that there will be multiple dots formed at one intersection point, depending on the pitch and width of the trench as summarized in figure 4. This is important because it suggests that complex nanodot arrays can be formed by engineering the surface topography.

Moreover, the pulse laser melting induced fragmentation of NIL defined metal nanogratings offers several advantages over other methods. First, this method inherits the high-throughput and low-cost nature of NIL. Second, with a single laser pulse of 20 ns, the high processing speed of our technique not only greatly reduces the processing time, but also offers negligible thermal effect on the substrates, enabling it suitable for different substrate materials including plastics. Third, the laser spot is adjustable in a certain range and step and repeat exposures can be achieved for wafer scale area. Fourth, the

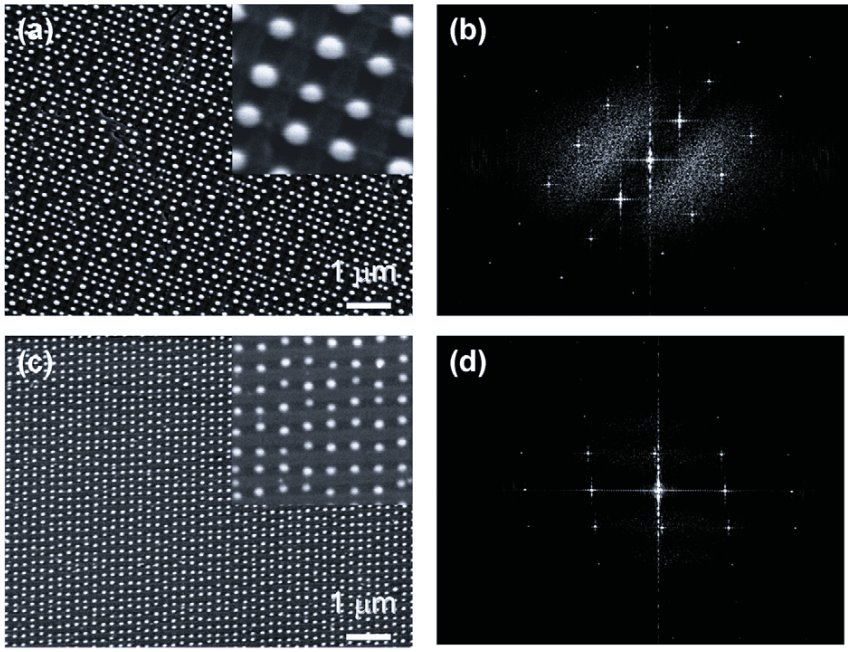

Figure 3. SEM and FFT images for regular Au and permalloy nanodot arrays on pre-patterned surfaces with shallow trenches. (a) Au nanodot arrays fabricated by fragmentation of Au gratings (200 nm pitch, 100 nm width, 10 nm thick, with 2 nm thick Ti as adhesion layer) on pre-patterned fused silica substrate. The dot size is 80.1 ± 8.1 nm. Laser fluence: 325 mJ cm^{-2}. (b) FFT image for (a). (c) Permalloy nanodot arrays fabricated by fragmentation of permalloy gratings (200 nm pitch, 70 nm width, 7 nm thick) on a pre-patterned 210 nm thick SiO_2 capped Si wafer. The dot size is 72.5 ± 6.8 nm. Laser fluence: 790 mJ cm^{-2}. (d) FFT image for (c). The substrates have trenches of 200 nm pitch, 70 nm linewidth which are 10 nm deep.

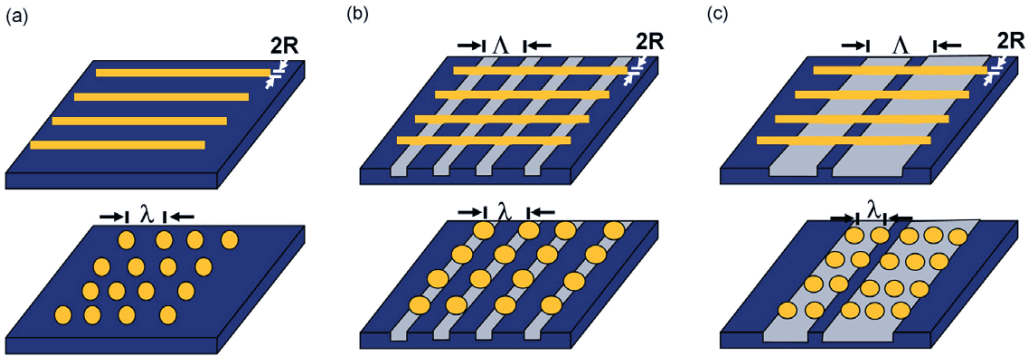

Figure 4. Summary of the relationship between the surface trench pitch and the resulting nanodot pitch. (a) For a flat surface, $\Lambda = \infty$, the pitch of the nanodot arrays along the original grating direction (λ) is about $2\pi R$, agreeing well with Rayleigh instability; (b) for the surface grating with a pitch $\Lambda < 2\sqrt{2}\pi R$, λ is determined by the trench pitch Λ, $\lambda = \Lambda$; (c) for the surface trenches with $\Lambda > 2\sqrt{2}\pi R$, $\lambda < \Lambda$, resulting in particle doublet (or triplet, etc) arrays.

geometries of the shallow trenches, or the geometries of the particle material, can be tuned separately, offering flexibility in the design of nanodot patterns. Finally, other substrate surface engineering methods such as the wettability difference in the difference area on a substrate might also be utilized to regulate the periodicity.

In summary, we proposed and demonstrated a novel method to fabricate regular metal nanodot arrays by laser fragmentation of metal nanogratings. This approach not only improved the particle size distribution, but also introduced periodicity along the original grating direction according to Rayleigh instability. The periodicity of the nanodot arrays was further engineered using a surface relief structure, resulting in a regular 2D array of nanodots with regular periodicity along both directions. As a simple fabrication method, it could be extended to other metals and has wide applications in many areas such as magnetics, plasmonics, surface enhanced Raman scattering and other photonic devices.

Acknowledgments

This work is supported in part by the US Defense Advanced Research Program Agency (DARPA) and the Office of Naval Research (ONR).

References

[1] Schmid G 1992 Large clusters and colloids—metals in the embryonic state *Chem. Rev.* **92** 1709–27

[2] Zhang W X 2003 Nanoscale iron particles for environmental remediation: an overview *J. Nanopart. Res.* **5** 323–32

[3] Fritzsche W and Taton T A 2003 Metal nanoparticles as labels for heterogeneous, chip-based DNA detection *Nanotechnology* **14** R63–73

[4] Sun S, Murray C B, Weller D, Folks L and Moser A 2000 Monodisperse FePt nanoparticles and ferromagnetic FePt nanocrystal superlattices *Science* **287** 1989–92

[5] So H-M *et al* 2003 Molecule-based single electron transistor *Physica* E **18** 243–4

[6] Wang Z C and Chumanov G 2003 WO_3 sol–gel modified Ag nanoparticle arrays for electrochemical modulation of surface plasmon resonance *Adv. Mater.* **15** 1285–9

[7] Leo G *et al* 2003 Ordering of free-standing co nanoparticles *Mater. Sci. Eng.* C **23** 949–52

[8] Chen S W 2001 Langmuir-blodgett fabrication of two-dimensional robust crosslinked nanoparticle assemblies *Langmuir* **17** 2878–84

[9] Alivisatos A P *et al* 1996 Organization of 'nanocrystal molecules' using DNA *Nature* **382** 609–11

[10] Zhang J P, Liu Y, Ke Y G and Yan H 2006 Periodic square-like gold nanoparticle arrays templated by self-assembled 2D DNA nanogrids on a surface *Nano Lett.* **6** 248–51

[11] Penn R L and Banfield J F 1998 Imperfect oriented attachment: dislocation generation in defect-free nanocrystals *Science* **281** 969–71

[12] Hicks E M *et al* 2005 Controlling plasmon line shapes through diffractive coupling in linear arrays of cylindrical nanoparticles fabricated by electron beam lithography *Nano Lett.* **5** 1066–70

[13] Lian J, Wang L, Sun X, Yu Q and Ewing R C 2006 Patterning metallic nanostructures by ion-beam-induced dewetting and Rayleigh instability *Nano Lett.* **6** 1047–52

[14] Chou S Y, Krauss P R and Renstrom P J 1995 Imprint of sub-25nm vias and trenches in polymers *Appl. Phys. Lett.* **67** 3114–6

[15] Chou S Y, Krauss P R and Renstrom P J 1996 Imprint lithography with 25-nanometer resolution *Science* **272** 85–7

[16] Xia Q F and Chou S Y 2008 Fabrication of sub-25 nm diameter pillar nanoimprint molds with smooth sidewalls using self perfection by liquefaction (SPEL) and reactive ion etching *Nanotechnology* **19** 455301

[17] Chou S Y and Xia Q F 2008 Improved nanofabrication through guided transient-liquefaction *Nat. Nanotechnol.* **3** 295–300

[18] Bosbach J, Martin D, Stietz F, Wenzel T and Trager F 1999 Laser-based method for fabricating monodisperse metallic nanoparticles *Appl. Phys. Lett.* **74** 2605–7

[19] Kawasaki M and Hori M 2003 Laser-induced conversion of noble metal-island films to dense monolayers of spherical nanoparticles *J. Phys. Chem.* B **107** 6760–5

[20] Wenzel T, Bosbach J, Goldmann A, Stietz F and Trager F 1999 Shaping nanoparticles and their optical spectra with photons *Appl. Phys.* B **69** 513–7

[21] Yang D Q, Meunier M and Sacher E 2004 Excimer laser manipulation and pattering of gold nanoparticles on the SiO_2/Si surface *J. Appl. Phys.* **95** 5023–6

[22] Image Pro Plus http://www.mediacy.com

[23] Xia Q F 2007 Nanostructure engineering using pulsed laser and nanoimprint lithography *PhD Thesis* Princeton University

[24] Rayleigh L 1878 On the instability of jets *Proc. Lond. Math. Soc.* **10** 4–13

[25] Nichols F A and Mullins W W 1965 Surface- (interface-) and volume-diffusion contributions to morphological changes driven by capillarity *Trans. Metall. Soc. AIME* **233** 1840–8